

Increasing salinity sequentially induces salt tolerance responses in Szarvasi-1 energy grass

Vitor Arcoverde Cerveira Sterner^{a,b}, Kristóf Jobbágy^{a,c}, Brigitta Tóth^d, Szabolcs Rudnóy^a, Gyula Sipos^e, Ferenc Fodor^{a,*}

^a Department of Plant Physiology and Molecular Plant Biology, ELTE Eötvös Loránd University H-1117 Budapest, Hungary

^b Doctoral School of Environmental Sciences, ELTE Eötvös Loránd University H-1117 Budapest, Hungary

^c Doctoral School of Biology, ELTE Eötvös Loránd University H-1117 Budapest, Hungary

^d Institute of Food Science, Faculty of Agricultural and Food Sciences and Environmental Management, University of Debrecen H-4032 Debrecen, Hungary

^e Agricultural Research and Development Institute H-5540 Szarvas, Hungary

ARTICLE INFO

Keywords:

Elymus elongatus subsp. *ponticus*
Tall wheatgrass
Salt stress
Sodium chloride

ABSTRACT

Soil salinity causes severe physiological disorders, decline in biomass, and crop production worldwide becoming more critical with global climate change. Consequently, salt-tolerant varieties received major focus in all sectors of agriculture. Biomass plants such as Szarvasi-1 energy grass (*Elymus elongatus* subsp. *ponticus* cv. Szarvasi-1) may play an important role in energy production if they are tolerant to environmental stresses. In this study, Szarvasi-1 energy grass has been investigated to reveal its tolerance to 50–200 mM NaCl in hydroponics. Significant decline in stomatal conductance appeared at 100 mM NaCl treatment but fresh and dry weight and the maximal quantum efficiency of PSII decreased only at 200 mM NaCl. Relative water content and total chlorophyll concentration did not change compared to the control. Leaf water potential was maintained at the control level for one week NaCl exposure, decrease became significant only after two weeks. Malondialdehyde concentration did not refer to oxidative stress. In the element composition of the plants, remarkable increase was found only for Mo whereas Ca, K, S, P, Mn decreased compared to the control. K to Na ratio remained higher than one in the shoot even at 200 mM NaCl. Salt treatment caused temporal and concentration-dependent changes in the expression of genes in the phenylpropanoid pathway, Na transport, photosynthesis, and cellular protection and repair. Szarvasi-1 was found to be fairly tolerant to NaCl which induced a sequential response switching on vacuolar compartmentalization at 50 mM, Na efflux at 100 mM, and cellular protection and repair at 200 mM.

1. Introduction

Soil salinity induces one of the most widespread abiotic disorders in plant species, known as salt stress, occurring naturally in all continents and distinct ecosystems and affecting about 5–7 % of the world's arable land (Maathuis et al., 2014; Saccò et al., 2021). Although accumulation of salts naturally occurring in different geographical locations, anthropogenic activity may start to escalate it. Moreover, ongoing climate change also triggers relevant drivers of the process such as frequent droughts, heat-stress periods, underpinned evapotranspiration demands, increased air temperature, rising sea level, over-use of fertilizer and deforestation (Breckle, 2002).

Plant growth and development is profoundly affected by salinity, as

two main stresses take place. The soil osmotic potential will be altered by the increasing salt concentration, thus hampering water uptake by the roots causing hyperosmotic stress. Secondly, the sodium ion content within the plant might reach toxic levels affecting protein functions and thus the metabolism. The duration of exposition represents an important factor and similarly to drought stress, plants immediately reduce cell expansion in young root tips and leaves and then stomatal closure takes place as a consequence of the first effect of the stress. Toxicity within the tissues requires a longer exposition and predominantly affects older leaves, possibly triggering early senescence (Munns and Tester, 2008). Growth inhibition and death may start at 100–200 mM NaCl exposition in glycophytes (plants that cannot tolerate 200 mM NaCl or higher in the soil) (İbrahimova et al. 2021), and in vitro, 100 mM is enough to inhibit

* Corresponding author: Department of Plant Physiology and Molecular Plant Biology, ELTE Eötvös Loránd University, Pázmány Péter lane 1/c 1117 Budapest, Hungary.

E-mail address: ferenc.fodor@tk.elte.hu (F. Fodor).

<https://doi.org/10.1016/j.stress.2024.100572>

Received 12 February 2024; Received in revised form 14 August 2024; Accepted 19 August 2024

Available online 21 August 2024

2667-064X/© 2024 The Authors. Published by Elsevier B.V. This is an open access article under the CC BY-NC-ND license (<http://creativecommons.org/licenses/by-nc-nd/4.0/>).

protein synthesis (Blumwald et al., 2000).

The uptake of Na^+ and Cl^- ions interfere with that of other essential ions causing disturbance in the ion homeostasis (Isayenkov and Maathuis 2019). The hydrated ions of Na^+ and K^+ have many similarities, making it difficult to discriminate between them, establishing an important basis of Na^+ toxicity as several K^+ transport pathways can be used by Na^+ . Besides Na^+ ions may enter the cells via Non-Selective Cation Channels (Wani et al., 2020). Certain highly selective transporters might maintain a ratio between K^+/Na^+ binding, as the K^+ inward rectifying channels (KIRC) in *Arabidopsis thaliana* (Spalding et al., 1999), or the K^+ outward rectifying channels (KORC) in the case of barley (*Hordeum vulgare*) roots (Wegner and Raschke, 1994) being both voltage-dependent, can be considered the first line of strategies to avoid excessive Na^+ uptake.

The altered ion homeostasis may finally cause the inhibition of photosynthetic processes due to oxidative stress and the inhibition of greening i.e. etioplast-to-chloroplast transformation and chlorophyll accumulation (Isayenkov and Maathuis 2019; Ibrahimova et al. 2021; Söti et al., 2023).

Plants have developed a wide range of strategies to deal with abiotic stresses. Detoxification, regulating osmotic adjustments, maintenance of cationic/anionic balance, scavenging reactive oxygen species and solute synthesis are all identified strategies to deal with salinity exposition (Ondrasek et al., 2022). The mentioned distinct mechanisms might be aggregated into three simpler strategies: osmotic response, Na^+ translocation limitation, and tissue tolerance. Antiporters responsible for ion compartmentalization, such as Sodium/Hydrogen Exchanger 1 (NHX1) (Glenn et al., 1999), might be an important tolerance mechanism in several different plant taxa. Specific and well-adapted plants to saline environments, halophytes, do not only tolerate greater salt stress but thrive on constant dosages, whereas most other plants perish, however, cytosolic enzymes of both glycophytes and halophytes are equally sensitive to Na^+ toxicity, therefore at cellular level the K^+/Na^+ ratio must be maintained (Flowers et al., 2003). The signaling mechanism known as Salt Overly Sensitive (SOS), is one of the most important pathways when plants are facing salt stress. SOS1 is actually a Na^+/H^+ antiporter that removes excess Na^+ from the cell (Wani et al., 2020). In the case of wheat, the system maintains ion balance and cell homeostasis, beyond that, roles of SOS1, SOS2, and SOS3 indicate also root and shoot growth response towards the stress (Shakirova et al., 2003).

A tall wheatgrass cultivar, Szarvasi-1 energy grass (*Elymus elongatus* subsp. *ponticus* (Podp.) Dorn; syn. *Thinopyrum obtusiflorum* (DC.) Banfi cv. Szarvasi-1) has been developed for biomass production as a renewable energy source (Csete, 2011; Martyniak et al., 2017) and as a potential plant for phytoremediation purposes (Rév et al., 2017; Vashegyi et al., 2011). It has been studied to reveal its heavy metal tolerance/sensitivity and was found to be relatively sensitive to Cd and Cu, tolerant to Ni and Pb, and an accumulator of Zn (Sipos et al., 2013; Kolberg et al., 2022). It has also been reported to be tolerant to drought, flooding and high soil salt concentrations but experimental details are missing on tolerated salt types and concentrations (Csete et al., 2011).

Aiming to test Szarvasi-1 under NaCl exposure, a series of experiments were conducted in hydroponics to describe its physiological tolerance in comparison with its element uptake and accumulation patterns as well as the expression pattern of genes related to salt stress responses. We hypothesised that this plant may have a well developed tolerance scheme due to wide adaptability to environmental stresses. To help reveal such mechanisms multivariate data analysis was performed to compare different results and discover correlations.

2. Materials and methods

2.1. Plant material and treatments

Before germination, uniform and healthy Szarvasi-1 seeds were selected and sterilized in 3 % (w/V) sodium hypochlorite solution for 15

min and washed thoroughly afterward. The selected seeds were placed on wet filter papers inside Petri dishes, under room temperature and sunlight exposed for one week. Thereafter, three plantlets with tillers measuring between 2 and 5 cm were grouped and rolled inside a 2 cm wide sponge-rubber strip and fastened into 35 mm diameter holes in polystyrene plates. Each plate containing 9 groups of plantlets were placed in plastic buckets filled with 5 dm³ quarter-strength Hoagland nutrient solution of the following composition: 1.25 mM KNO₃; 1.25 mM Ca(NO₃)₂; 0.5 mM MgSO₄; 0.25 mM KH₂PO₄; 11.6 μM 3B₃O₃; 4.5 μM MnCl₂·4H₂O; 0.19 μM ZnSO₄·7H₂O; 0.12 μM Na₂MoO₄·2H₂O; 0.08 μM CuSO₄·5H₂O and 25 μM Fe(III)-citrate-hydrate (Merck). This setup was maintained for two weeks and after the nutrient solution volume was doubled. The solutions of all buckets were changed weekly and were constantly aerated, the buckets were placed in the climate-controlled growth chamber at 20–25°C, at 70 % relative humidity and 150 μmol m⁻² s⁻¹ photosynthetic photon flux density (PPFD) with 10–14 h dark/light period.

After 1 week of germination and 4 weeks of pre-cultivation, the plants still wrapped together in the rubber sponge were transferred to smaller (8 cm in diameter) polystyrene rings, each with 3 plantlets were placed into 0.8 dm³ pots filled up with the same nutrient solution but supplied with NaCl at 50, 100 and 200 mM concentrations. One experiment made up a total of 18 pots consisting of 3 control pots (no NaCl added), and 5 pots within each mentioned concentration referred to as Na50; Na100, and Na200.

2.2. Physiological and elemental analysis

2.2.1. Determination of the relative water content

After 14 days of treatment all plants were harvested. The relative water content (RWC) analysis was carried out with samples cut from the first fully developed leaves. Approximately twenty mg samples were taken (three samples from each pot). The fresh weight (FW) was measured and after, all samples were incubated inside Petri dishes on filter papers saturated with deionized water for 2 h and the weights were measured again every hour, in a total of 4 h to ensure the full hydration of the tissue, turgid weight (TW) was then carried out. The samples were put into a dryer overnight at 85 °C after all the previous processes, to reach full dehydration and constant dry weight (DW). The relative water content was calculated based on the equation:

$$RWC (\%) = \frac{(FW - DW)}{(TW - DW)} \times 100$$

2.2.2. Mass measurement

The roots were cut and rinsed with deionized water to remove traces of nutrient solution, then centrifuged between filter papers at 300 g and weighed to determine FW. The dry mass of all tissues (shoots and roots separately) was determined after drying at 80 °C for 24 h.

2.2.3. Stomatal conductance

Stomatal conductance was measured with an AP4 porometer (DELTA-T Devices, Cambridge, UK) on the middle sections of the youngest fully developed leaves (adaxial epidermis), after 7 and 14 days of treatment. Transpiration was calculated as mmol H₂O m⁻²s⁻¹. Each measurement was carried out three times on three individual plants in each treatment group.

2.2.4. Water potential

Water potential in the youngest fully developed leaves was measured by thermocouple hygrometry using a Wescor H-33T Dew-point Microvoltmeter (Wescor Inc., West Logan, Utah, USA). The leaf samples were first acclimated simultaneously in 10 Wescor C52 sample chambers for 3 h of gas phase equilibration to reach content reading. Each set of measurements consisted of two samples from each treated group, triplicated. Measurements were performed at 7, 10, and 14 days after the NaCl

exposition started.

2.2.5. Chlorophyll *a* fluorescence induction

Chlorophyll (Chl) *a* fluorescence induction measurements were carried out in vivo with a PAM 101–102–103 Chl Fluorometer (Walz, Effeltrich, Germany) at harvest. Dark adaptation was induced for 15 min and F_0 was determined by switching on the measuring light (modulation frequency of 1.6 kHz and PFD less than $1 \mu\text{mol m}^{-2}\text{s}^{-1}$). Illumination with far-red light was applied for 2 s in order to eliminate reduced electron carriers (Belkhdja et al., 1998). Maximum fluorescence yield of the dark-adapted stage, F_m was measured by applying a 0.7 s pulse of white light (PPFD of $3500 \mu\text{mol m}^{-2}\text{s}^{-1}$, light source: KL 1500 electronic, Schott, Mainz, Germany). The maximal quantum efficiency of photosystem (PS) II centres was calculated as:

$$\frac{F_v}{F_m} = \frac{F_m - F_0}{F_m}$$

2.2.6. Chlorophyll concentration

The determination of Chl concentration was performed according to Porra et al. (1989) at harvest. Leaf samples of 25 mg from the youngest fully developed leaves were homogenised in 80 % (V/V) acetone. Samples were then centrifuged at $10,000 \times g$ for 5 min. The supernatant was extracted, and quantification of Chl *a* and *b* was carried out based on known absorption peaks, using a spectrophotometer (UV-2101 PC, Shimadzu, Japan).

2.2.7. Malondialdehyde concentration

Lipid peroxidation was assessed by measuring the malondialdehyde (MDA) concentration according to Heath and Packer (1968) at harvest. Leaf samples of 100 mg were homogenised in 1 ml 0.1 % (w/V) trichloroacetic acid and centrifuged at $15,000 \times g$ for 15 min at 4°C . The supernatant was collected and equal volumes of 20 % (V/V) trichloroacetic acid and 1.0 % (w/V) thiobarbiturate was added, solutions were incubated at 90°C for 60 min. The MDA concentration was determined by measuring absorption at 532 nm ($\epsilon = 155 \text{ mM}^{-1}\text{cm}^{-1}$) of both shoots and roots.

2.3. Elemental analysis

Samples of 500 mg were collected for element content determination of roots and the shoots, both dried in a dryer at 85°C for 48 h. Pre-digestion starts as cc. H_2O_2 was added to the flask containing samples for 1 h. After, cHNO_3 is added for 15 min at 60°C increased to 120°C for further 45 min. The solutions were left to cool off and finally the volume was made up to 10 cm^3 . The solution was homogenized and filtered through MN 640 W filter paper (Macherey-Nagel, Düren, Germany). ICP-OES (inductively coupled plasma–optical emission spectrometer, Spectro Genesis, SPECTRO, Freital, Germany) was the equipment used for elemental content determination of the filtrate. A multielement standard was used for calibration (Loba Chemie Product code: I166N, Loba Chemie PVT, Mumbai, India) for a total of 33 elements. All samples were prepared in triplicate.

2.4. Identification of sequences of interest and designing oligonucleotide primers

Since the genome of none of the already sequenced *Thinopyrum* species are annotated, the sequences of interest (SOI) were accessed using expressing sequence database of the diploidic *Aegilops tauschii* subsp. *strangulata*, closest annotated relative of the genus *Thinopyrum*, in NCBI (<https://www.ncbi.nlm.nih.gov/>). SOIs were blasted against *Thinopyrum elongatum* reference genome ASM1179987v1 (GenBank ID: GCA_011799875.1) to verify them in the *Thinopyrum elongatum* genome. Photosystem II protein D2 sequence was accessed as translated protein of *Thinopyrum elongatum* that was applied as template. In order to study

the relative transcript abundances, oligonucleotide primers were designed using Primer 3 (Untergasser et al., 2012), T-Coffee (Higgins and Heringa, 2000), Clustal Omega (Sievers and Higgins, 2021), and Oligo Analyzer (Teemu Kuulasmaa) softwares on the *Aegilops* sequences. The design was corrected based on the *Thinopyrum* genome assembly. Data of the blast results and the oligonucleotide primers are listed in Supplementary Table S1. Reaction efficiencies of the designed oligonucleotide pairs were obtained from the LinRegPCR software (Ramakers et al. 2003).

2.5. Quantitative real-time polymerase chain reaction based analysis of transcript abundances

Sampling of the youngest fully developed leaves took place on the 8th hour, 3rd day, 7th day, and 14th day after treatment. To isolate total RNA, Direct-zol RNA Miniprep Kits (Zymo Research, Irvine, CA, USA) was applied according to the manufacturer's instructions. Copy DNA (cDNA) was transcribed using random hexamer oligonucleotide primers in the Thermo Scientific RevertAid Kit. qRT-PCR reactions were run on an ABI StepOnePlus Real-Time PCR instrument (Thermo Fisher Scientific), using Maxima SYBR Green/ROX qPCR Master Mix (Thermo Fisher Scientific). In order to normalize the relative transcript abundances, *Cell Division Control 48* (Ta54227; Paolacci et al., 2009), *Glyceraldehyde 3-phosphate Dehydrogenase 2* (GAPDH2) and *Actin 3* (Kiarash et al., 2019) were used (oligonucleotide primers are listed in Supplementary Table S1). The geometric mean of the C_t values of the references was applied for normalization. Relative transcript abundances of the SOIs were calculated according to Pfaffl (2004).

2.6. Statistical analysis

The experiments were repeated three times, and as mentioned, all sampling and analysis were carried out in triplicate. ANOVA + Tukey multiple range test were used for the analysis of variance and proof of actual (significant) difference between the resulting effects of the applied treatments, performed on Origin Software (Origin (Learning Version), Version 2022b. OriginLab Corporation, Northampton, MA, USA.)

2.6.1. Principal component analysis

For multivariate data relationship exploration, Principal Component Analysis (PCA) was applied, which creates a new coordinate system based on variance analysis, preserving original data point positions to maximize variation with fewer components. Choosing the component count relies on interpreting the scree plot and positive Eigenvalues. Eigen decomposition of a symmetric positive semidefinite matrix generates a new orthogonal basis that reveals linear relationships between variables, according to the angle of interaction between the parameters, as 0° degrees indicates perfect positive correlation, 180° a perfect negative correlation and 90° degrees indicates no linear correlation (Podani, 2000).

Considering plants under different treatments and the different measurements of physiological status, elemental composition, and gene expression, PCA based on a correlation matrix standardizes variables for equalized analysis, as many of the parameters would belong to different types of numerical scales. The resulting graphs known as Rohlf biplots display objects (plants under different treatments) as dots and variables as vectors starting with the origin of the orthogonal system and showing possible correlations between variables. The mentioned vectors are named according to their specific acronym, and the objects are named K1; K2; and K3 for control, and A1-A5 for Na50, B1-B5 for Na100 and C1-C5 for Na200, indicating the different treatments. Clusters of specimens under similar treatments might be created, indicating that such individuals would have similar responses at genetic, elemental, and physiological levels. On the left and bottom axes, the scree plot analyses are represented.

3. Results

3.1. Physiological responses to NaCl treatments

The treated plants started to present visible morphological symptoms after 5 days of exposure, smaller and yellowish leaves started to appear only at the highest concentration (Na200), but it did not overwhelm the plant's tolerance as none of the individuals withered completely nor died. After 14 days of exposure, symptoms were clear in shoots and treatments showed a gradient decrease in size, further yellowing at Na100 and senescence of some leaves at Na200, however, only shoots reached a significant difference in both fresh and dry weight (Fig. 1). When comparing dry weight, a decrease of 40.11 % between control and Na200 was measured (Fig. 1B).

Sampled tissues of the first fully developed leaves were analysed for relative water content (RWC) and water saturation deficit (WSD) on the 14th day. The statistical analysis showed no significant difference between the different treatments, as observed in Fig. 1C and D.

The pH of the nutrient solutions decreased slightly as the NaCl concentration was increased. After 14 days of exposition period, pH was measured again and it was found that it reached a slightly alkaline level. Only Na200 had a significantly lower value of pH 7.25 (Table 1).

Stomatal conductance was measured at 7 and 14 days of exposition. Variation between individuals under the same treatment generated a considerable standard deviation, the overall trending behavior, however, remained a clear decrease of stomatal conductance as the NaCl concentration was increased. If control plants are compared with Na200, 7 days of exposure showed a 73 % stomatal conductance decrease, and

Table 1

pH measurements of fresh bulk nutrient solution and 14 days later, at the harvest day. Data are presented as mean \pm SD ($n = 5$). Significant differences between the treatment groups are indicated by different letters. (One-way ANOVA with Tukey-Kramer post hoc test, $p < 0.05$).

Treatment (mM NaCl)	pH (fresh solution)	pH (harvest day)
0	6.14	7.40 \pm 0.01 a
50	5.76	7.46 \pm 0.06 a
100	5.32	7.29 \pm 0.16 a
200	5.11	7.25 \pm 0.02 b

with 14 days of exposure, a decrease of 74.7 %. However, the difference was not significant at 7 days just after 14 days (Fig. 2A).

Water potential was measured at 7, 10, and 14 days after NaCl exposition was initiated. Two different patterns were observed between the three measurements: 7 days of exposition showed a slight but non-significant increase (14.15 %) in water potential with the increasing NaCl concentration. On the contrary, at 10 and 14 days of exposition, a gradually decreasing trend in water potential was measured becoming significant at Na100 and Na200 at 14 days of exposure (Fig. 2B).

Chlorophyll *a* fluorescence induction was performed to assess the maximum quantum efficiency of photosystem II. At 14 days of stress exposure, a decreasing trend was observed with the increasing NaCl concentration from the healthy 0.82 level to the slightly stressed 0.75 value (Fig. 2C).

Treated plants had a minor increase in total Chl concentration, reaching a maximum of 34 % increment when comparing the control

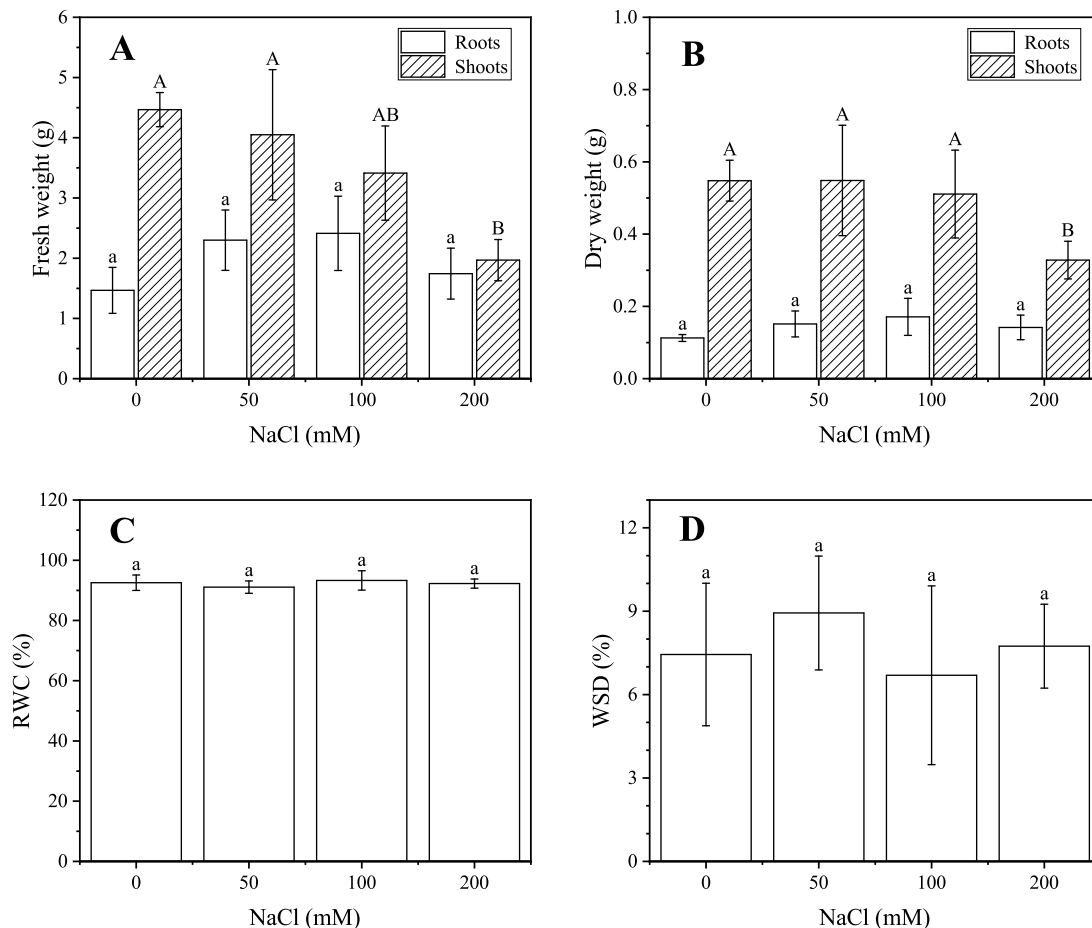


Fig. 1. Fresh (A) and dry weight (B) of the roots and shoots and relative water content (C) and water saturation deficit (D) of the youngest fully developed leaves of Szarvasi-1 energy grass. Data are presented as mean \pm SD ($n = 5$). Significant differences between the treatment groups are indicated by different letters. (One-way ANOVA with Tukey-Kramer post hoc test, $p < 0.05$. Lowercase and uppercase letters indicate independent analysis.).

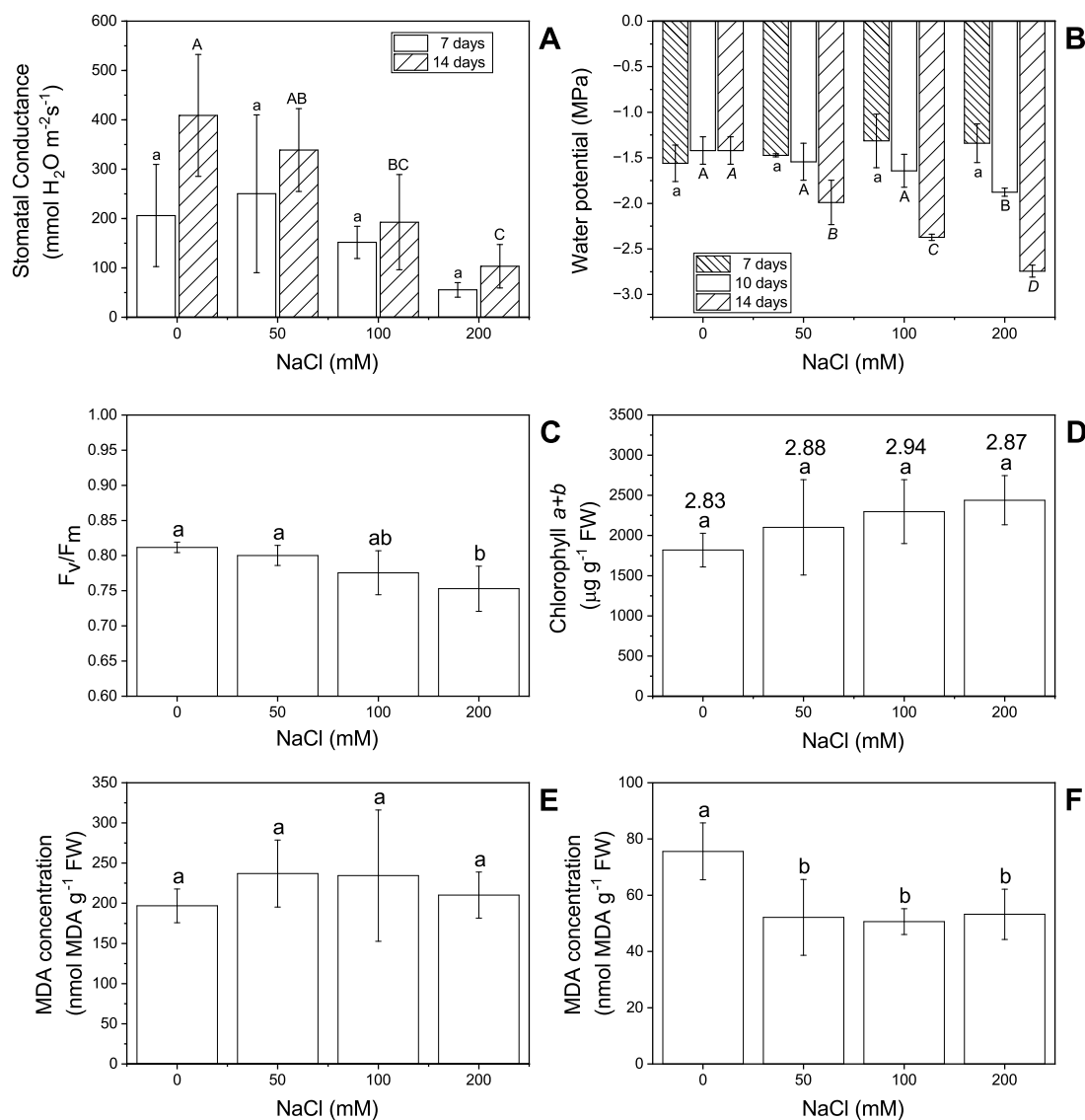


Fig. 2. Stomatal conductance (A), water potential (B), maximum quantum efficiency of PSII reaction centers (C), Chl *a* + *b* concentrations (with Chl *a*/*b* ratio indicated on top of each column) (D) of the youngest fully developed leaves and malondialdehyde concentration in the roots (E) and the youngest fully developed leaves (F) of Szarvasi-1 energy grass. Stomatal conductance was measured at 7 and 14 days while water potential at 7, 10, and 14 days of exposure to different concentrations of NaCl. Data are presented as mean \pm SD ($n = 5$). Significant differences between the treatment groups are indicated by different letters. (One-way ANOVA with Tukey-Kramer post hoc test, $p < 0.05$. Lowercase, uppercase and italic letters indicate independent analysis.).

with Na200, but none of the groups in this experiment showed a significant difference (Fig. 2D). The ratio between Chl *a* and *b* had an insignificant variation around 2.8.

Malondialdehyde content determination of shoots and roots was performed after 14 days of treatment. Concerning the roots, slightly higher MDA concentration was measured when compared to shoots (Fig. 2E). Significant difference among the treated groups was only evident in shoot MDA concentration and only between control and all other treated groups, otherwise, no significant difference was found (Fig. 2F).

3.2. Changes in the ionic profiles

Elemental constitution of shoots and roots was assayed from samples on the 14 days of NaCl exposure. The concentration of the measured elements can be seen in Supplementary Table S2 and S3 whereas heat-maps showing elemental variation of the shoots and roots compared to the control are shown in Fig. 3A. Considering the shoots, molybdenum had a very intense increase in Na100 and Na200 treatments compared to

the control, while iron and copper also increased with increasing NaCl concentration. On the opposite side: sulfur, phosphorus, manganese, potassium, and calcium showed a decrease under NaCl treatment. In the roots, only molybdenum increased whereas most of the other analysed elements had a considerable decrease.

The potassium-to-sodium ratio showed a decreasing trend in both shoots and roots. However, only the control values were significantly different from those of treated plants as there was a major drop by two orders of magnitude (Fig. 3B). It must be noted that Szarvasi-1 maintained a K to Na ratio higher than one in the shoot even at Na200 treatment.

3.3. Responses at the level of gene expression

From the investigated genes affecting the phenylpropanoid pathway *Chalcone Synthase (CHS)* did show a greatly variable response affected by both time and NaCl concentration with the greatest increase in expression, in Na200 on the 14th day (Fig. 4, Supplementary Figure S4). *Cinnamyl Alcohol Dehydrogenase 5 (CAD5)* did show a more similar

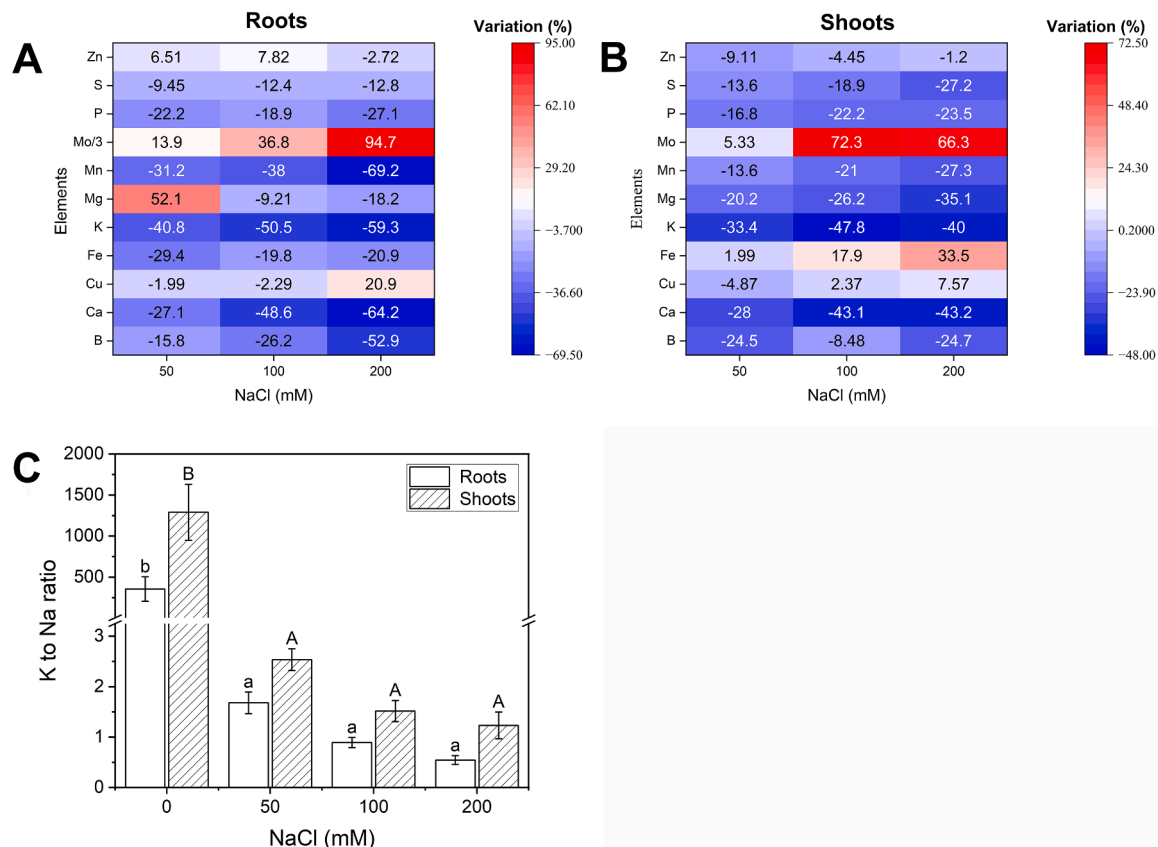


Fig. 3. Heatmap of elemental variation in the roots (A) and shoots (B) of Szarvasi-1 energy grass exposed to different NaCl concentrations with untreated control plants as baseline. Potassium to Sodium ratio in the roots and shoots of Szarvasi-1 energy grass exposed to different NaCl concentrations (C). Statistical analysis for A and B was performed on the raw data ($n = 5$) shown in Supplementary Table S2 and S3. For C, data are presented as mean \pm SD ($n = 5$). Significant differences between the treatment groups are indicated by different letters. (One-way ANOVA with Tukey-Kramer post hoc test, $p < 0.05$. Lowercase and uppercase letters indicate independent analysis).

expression curve between treatments, with the highest expressions on the 14th day as well. Dihydroflavonol 4-reductase (*DFR*) exhibited the most extreme fold changes – both in regards to overexpression and underexpression – from all the genes, where the former was prominent in the 8-hour and 3-day samples and the latter in the 7-day and 14-day samples.

Mitogen-activated Protein Kinase 6 (MAPK6) did exhibit a universal underexpression and a similar expression pattern in all the samples except Na50 where it was overexpressed at the 8th hour (Fig. 4, Supplementary Figure S4). *NHX1* expression was greatly affected by both time and treatment, although it is worth mentioning that Na200 was an exception here since it did show a constant underexpression the whole time. *Salt Overly Sensitive 1 (SOS1)*, similar to *NHX1*, exhibited highly variable expression patterns, with the greatest increases in the Na200 groups.

Genes affecting photosynthesis did yield intriguing results (Fig. 5, Supplementary Figure S4). The expression of *Oxygen-evolving Enhancer 1 (PSBO)*, *D2 (PSBD)* and *CP43 (PSBC)* were somewhat lower at 8 h under the 100 and 200 mM NaCl treatment compared to the control. In subsequent sampling times the expression of these genes recovered to control level or exceeded it (*PSBO* and *PSBD*). *Serine Hydroxymethyltransferase 1 (SHM1)* on the other hand did show highly diverse expression patterns, with the highest upregulation on the 7th day. *Pheophorbide a Oxygenase (PAO)* did exhibit an overexpression during almost the whole experiment, most prominent in the Na100 and Na200 groups.

Heat Stress Transcription Factor A-1 (HSFA1) expressions were rather mildly affected regarding treatment and time as well, although the expression patterns did exhibit a noticeable divergence (Fig. 5,

Supplementary Figure S4). *Heat Shock 70 kDa (HSP70)* was upregulated in almost all the cases, at most extreme in Na200 on the 8th hour. *Cellulose Synthase A catalytic subunit 1 (CESA1)* did yield similar expression patterns, with overexpression at the 8-hour samples and control level or underexpression in all the later samples.

3.4. Relationships between physiological, elemental, and genetical responses

A PCA was performed for roots and shoots independently but as gene expression measurements were done only with shoot tissues the root plot contains only the physiological parameters and ionomics data (Figs. 6). Observing the studied objects, the formation of clusters is seen between the control and treated plants (see red dots representing each treatment group) in both roots and shoots. The control group is highly separated in both plots but the NaCl treatment groups separate only in the shoot showing distinct characteristics based on the analysed parameters. Sodium vectors show a positive correlation with all NaCl treatments in the root whereas a strong positive correlation in the shoot was found only with Na100 and Na200. Interestingly, NaCl shows a positive correlation also with the fresh and dry weight and the Mo vectors. The rest of the elements are better correlated with the control group.

In the shoot, the control group had a positive correlation with MDA concentration and most of the elements except for Mo, Cu, and Fe. Among genes, *DFR* had the strongest relationship with the control group but *CESA*, *PSBC*, and *MAPK6* also correlated well with this group. Increasing the NaCl concentration to 50 mM there is a transition in the correlation of physiological parameters (fresh and dry weight, water

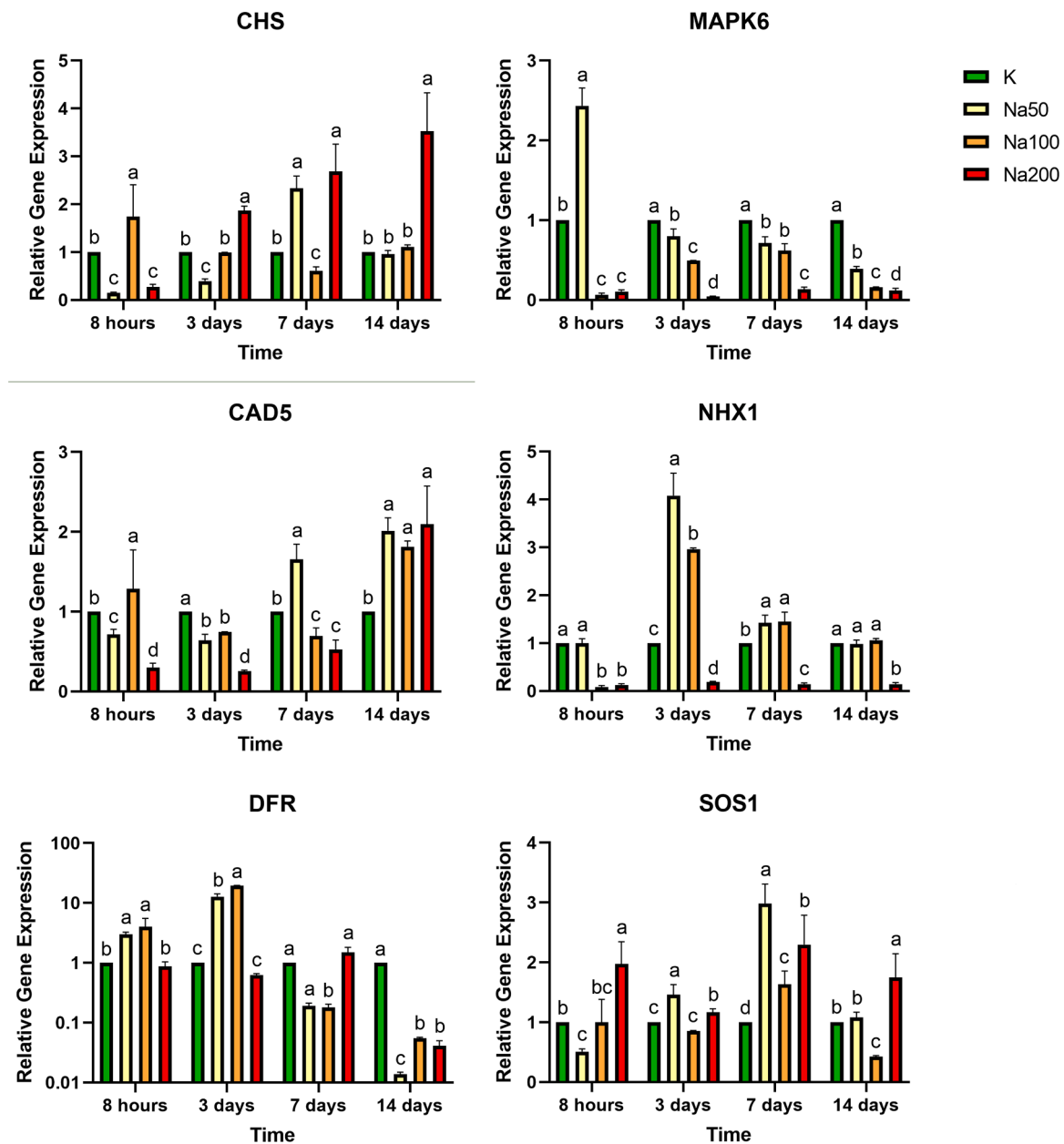


Fig. 4. Expression of *CHS*, *CAD5*, *DFR*, *MAPK6*, *NHX1* and *SOS1* genes in the leaves of Szarvasi-1 energy grass exposed to different NaCl concentrations. Sampling was done 8 h, 3, 7, and 14 days after the treatment. Data are presented as mean \pm SD ($n = 3$). Significant differences between the treatment groups are indicated by different letters. (One-way ANOVA with Tukey-Kramer post hoc test, $p < 0.05$).

potential, stomatal conductance, maximal quantum efficiency of PSII) to the Na50 group. The genes *NHX1* and *SHM1* showed a very significant positive correlation with this group. The Na100 treatment group correlated positively with *SOS1*, *CAD5*, *PAO*, and *HSP70* whereas the Na200 group was closely correlated with *CHS*, *PSBO*, *PSBD*, and *HSA1* but showed a good correlation with *HSP70* as well.

4. Discussion

Szarvasi-1 energy grass was claimed to be a salt-tolerant variety of tall wheat grass but there was a lack of experimental evidence to confirm it (Csete et al., 2011). In this study, an increasing load of NaCl was applied in nutrient solution to test physiological tolerance, element distribution profile changes, and genetic responses. The plant exhibited a significant physiological tolerance, only the Na200 treatment caused the decline in fresh and dry weight and the maximal quantum efficiency

of PSII. Nevertheless, the latter decreased only slightly below the control level. In the meantime, a slight increasing trend was observed in $\text{Chl } a + b$ with increasing NaCl concentration which can be explained by the decreasing fresh weight referring to unaffected Chl synthesis but hindered shoot growth. These observations are by decreasing water potential in the leaves which became significant with treatment time and increasing NaCl concentration. Change in water relations is also shown by the stomatal closure that became significant after two weeks of Na200 treatment time. Similar changes were found in wild barley (Kiani-Pouya et al., 2020), and four wheat genotypic variations, but with lower concentrations of NaCl, as 100 mM could already trigger such responses in sensitive cultivars (Ouerghi et al., 2000).

A high concentration of NaCl in the growth medium inevitably causes changes in the elemental composition of the roots and consequently of the shoots. Decreases of most essential elements (K, Ca, Mg, P, S, and Mn) were detected in Szarvasi-1 and have also been found in wild

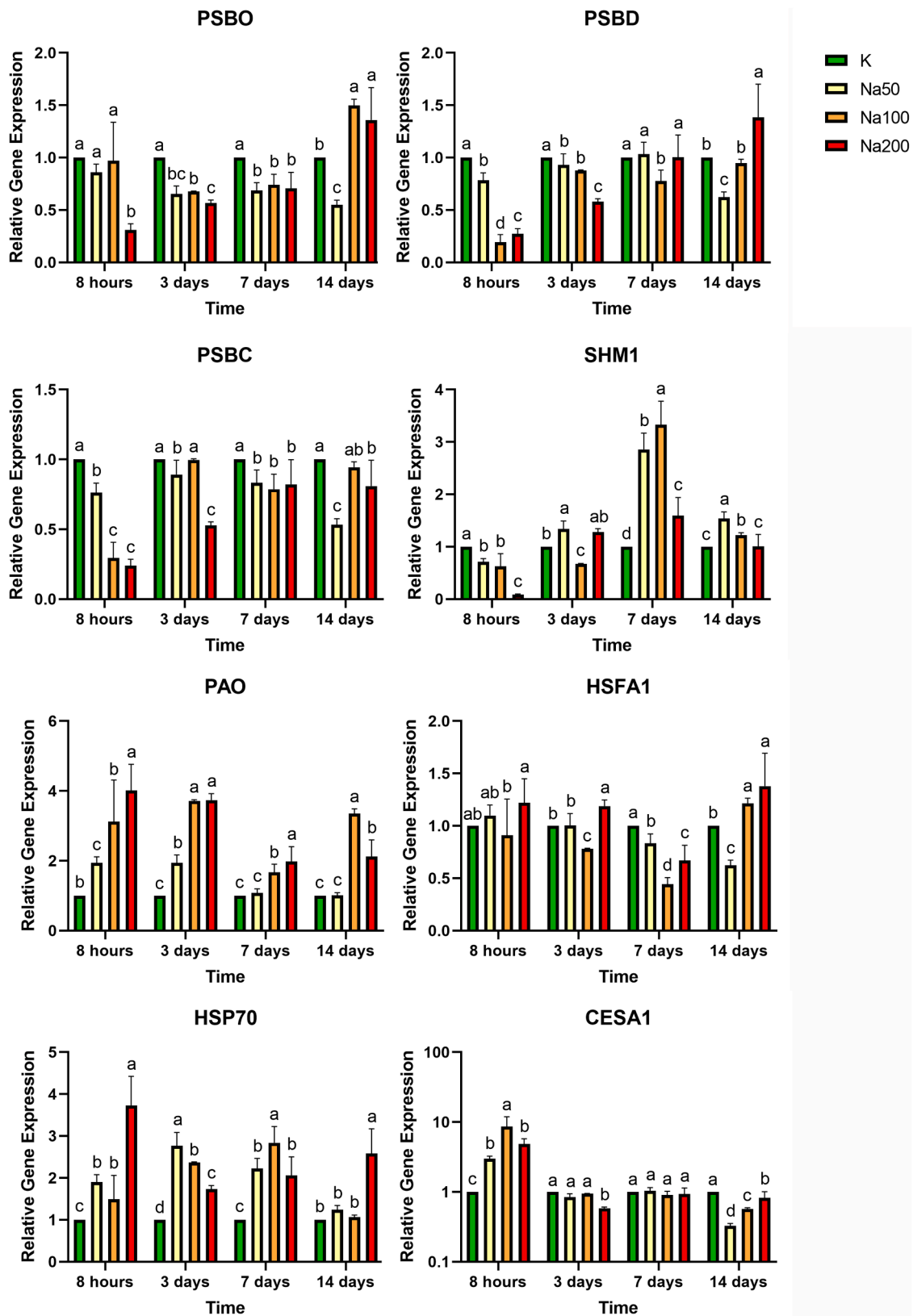


Fig. 5. Expression of *PSBO*, *PSBD*, *PSBC*, *SHM1*, *PAO*, *HSFA1*, *HSP70* and *CESA1* genes in the leaves of Szarvasi-1 energy grass exposed to different NaCl concentrations. Sampling was done 8 h, 3, 7, and 14 days after the treatment. Data are presented as mean \pm SD ($n = 3$). Significant differences between the treatment groups are indicated by different letters. (One-way ANOVA with Tukey-Kramer post hoc test, $p < 0.05$).

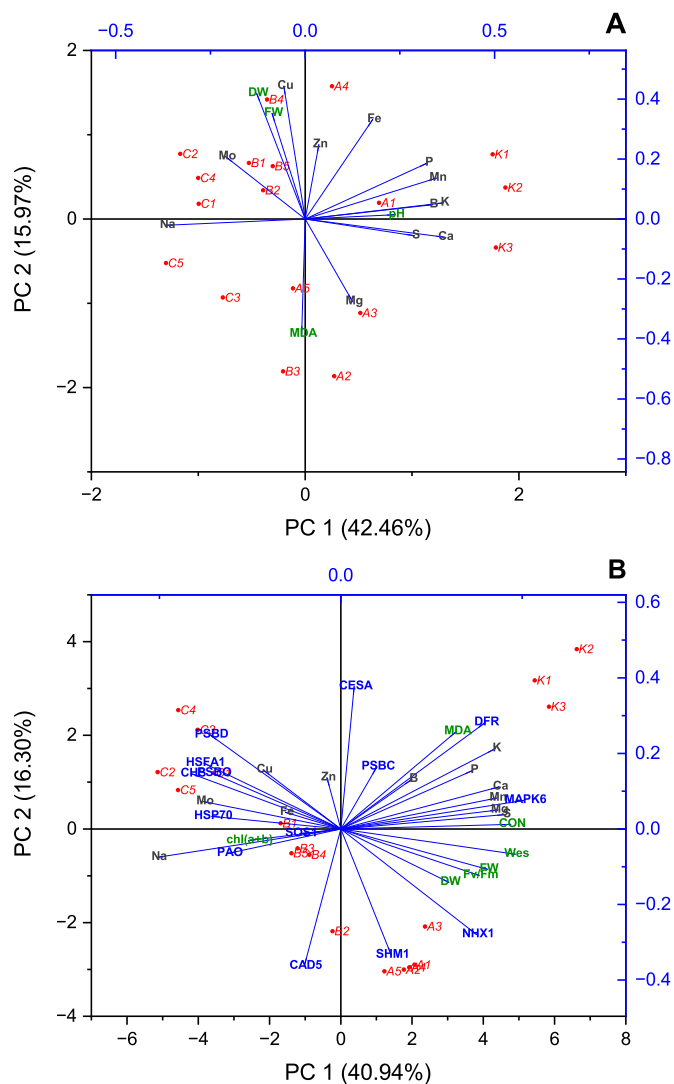


Fig. 6. Principal component analysis of the energy grass roots (A) and shoots (B) (Rolfh Biplot). Roots, objects (red): control, K1–3; A1–5 Na50; B1–5, Na100; C1–5, Na200. Variables (blue lines): physiological parameters (pink) as MDA (malondialdehyde concentration); DW and FW (dry and fresh weight); pH of the nutrient solutions; elements (gray) as Na, K, Ca, Mg, S, P, B, Mn, Zn, Mo, Cu. Shoots, objects (red): control, K1–3; A1–5 Na50; B1–5, Na100; C1–5, Na200. Variables (blue lines): physiological parameters (pink) as MDA (malondialdehyde concentration); DW and FW (dry and fresh weight); Chl(a + b); CON (stomatal conductance); Fv/Fm (maximal quantum efficiency of PSII); WES (water potential); RWC (relative water content); pH of the nutrient solutions; elements (gray) as Na, K, Ca, Mg, S, P, B, Mn, Zn, Mo, Cu; gene expression (blue) as *CESA*, *PSBC*, *DFR*, *MAPK6*, *NHX1*, *SHM1*, *CAD5*, *SOS1*, *PAO*, *HSP70*, *CHS*, *PSBO*, *HSFA1* and *PSBD*.

and cultivated barley (Wu et al., 2013). Salinity stress studies on maize show that Fe, Zn, and Cu uptake are not affected by salinity stress (Guo et al., 2017), and except for Fe and to a lesser extent Cu a similar trend is noticeable in Szarvasi-1. Mo uptake had a positive correlation with Na in both shoots and roots of Szarvasi-1. As Mo is supplied as Na salt in the nutrient solution, it might have an uptake co-stimulation but we have not found any other previously established explanations in the literature.

The K to Na ratio in Szarvasi-1 was very high in the control plants which is understandable as the control nutrient solution contained only 0.24 μM Na as compared to 1.5 mM K. When NaCl was introduced in the solution the ratio dropped but remained above one in the shoot even at Na200 reflecting a highly preserved K uptake and allocation under Na

predominance. As a reference, the well-known salt-tolerant energy reed (*Arundo donax*) leaves had a 0.5 K to Na ratio at 200 mM alkaline salt treatment (Müller et al., 2022). On the other hand, based on the data presented here Szarvasi-1 has a K/Na discrimination character between *H. vulgare* L. and *T. aestivum* cv. Chinese Spring (Gorham et al., 1990). In salt-tolerant genotypes of barley (*Hordeum vulgare*), it was found that several mechanisms are responsible for salinity tolerance including better control of membrane voltage, higher H^+ pump activity, more efficient Na^+ efflux from the cytosol and higher sensitivity to added Ca^{2+} (Chen et al., 2007). In Szarvasi-1, possibly an efficient accumulation of K is coupled with similarly efficient Na efflux as the K concentration dropped only to 50–30 % of the control while Na concentration hardly doubled from Na50 to Na200 in root and shoot tissues.

Salinity induces a series of adjustments in all plants to cope with high concentrations of Na^+ ions and the osmotic stress caused by them. The altered expression of genes aims to maintain cellular homeostasis by preserving K uptake and accumulation, decreasing Na uptake as well as facilitating Na efflux or compartmentalizing Na in the vacuole (Munns and Tester, 2008b). It is important to notice that the duration of stress exposition and the time of observation of responses by the plants are also very important parameters. In Szarvasi-1, the *NHX1* gene responsible for vacuolar transport of Na seems to be one of the first responses at low Na concentrations and it is gradually downregulated while *SOS1*, the plasma membrane Na^+/H^+ antiporter is switched on under higher Na concentrations.

MAPK6 is one of the main regulators during stress reactions, yet *MAPK6* expression (and *MAPK6* phosphorylation state) itself is also highly regulated. When it is phosphorylated, it activates (besides other things) an ethylene signaling cascade, which leads to increased ROS production, resulting in further stress (Li et al., 2014). Therefore its expression usually drops during abiotic stress conditions. This is what we have found in Szarvasi-1: a decreasing expression with increasing Na concentration. Furthermore, this may be the explanation for the decreased production of MDA, the by-product of lipid peroxidation, compared to control plants. The accumulation of MDA is well documented under oxidative stress in other plants such as maize (*Zea mays*), barley (*Hordeum vulgare*), and other grasses such as Kunth (*Chloris Gayana*) (Abdel Latif et al., 2019; Li et al., 2008; Luna et al., 2000).

Phenylpropanoids have a significant role in responses to stress such as high salinity (Petrucci et al., 2013). *CHS* is a potential indicator of the general activity of the phenylpropanoid (especially the flavonoid) pathway (Dao et al., 2011). We have found a positive response of this gene to increasing NaCl concentrations, especially with the time of exposure. Other components of the phenylpropanoid metabolism seem to be less affected such as *CAD5* or only affected by low and medium NaCl levels (Na50 and Na100) such as *DFR*. These latter enzymes are components of lignin and anthocyanin or tannin biosynthesis, respectively (Sanchez-Augayo et al., 2004; Petrucci et al., 2013; Tattini et al., 2006).

Under salinity stress, it is very important to preserve the intactness and functionality of the photosynthetic apparatus. Several genes were examined that are involved in the synthesis of major proteins such as *PSBD* (D2), *PSBO*, and *PSBC* (CP43). The expression of *PSBD*, *PSBO* and *PSBC* genes showed slight variation in time around the control level but it seems to be only a homeostatic adjustment to counterbalance metabolic changes under salt exposure as the damage of the photosynthetic apparatus was not confirmed by marked changes in either the maximal quantum efficiency of PSII or the Chl concentration.

HSP70 was described as a positive regulator of *SOS1* in *Arabidopsis thaliana* (Montero-Barrientos et al., 2010). *HSP70* overexpressing sugarcane plants also showed higher resistance against most types of abiotic stresses including salinity, manifesting itself by better germination rate, relative water content, Chl concentration, and maximum quantum yield than the wild type (Augustine et al., 2015). This gene showed overexpression in Na200 plants indicating the need for protection and/or repair. *HSFA1* is a central, mostly positive regulator of the system and

hsfa1 mutant *Arabidopsis thaliana* plants have smaller seeds, while they also exhibit slower germination rate and diminished growing rate. Their heat, salt, and oxidative stress tolerance is also significantly worse than the tolerance of the wild type (Liu et al., 2011). Nevertheless, this gene did not show a clear activation in NaCl-stressed Szarvasi-1 plants compared to the control.

The diverse data of gene expression, ionomics, and physiological parameters made it necessary to apply a bioinformatics approach to select the most important factors, find interconnections and provide an overall description of salt stress responses in Szarvasi-1 energy grass plants (Füzy et al., 2019). The good separation of treatment groups made it possible to identify the major variables i.e. physiological and ionic components changing with increasing NaCl concentration and the genetic components driving the changes. In the control plants, where the only Na source was the Na₂MoO₄ in 0.12 μM concentration, the plants grew well, and the osmotic balance was maintained by K. The ionic composition of the shoots changed antiparallel with Na i.e. increasing NaCl triggered decreasing element uptake which is in correlation with decreasing dry weight. The genes *DFR*, *PSBC*, *CESA1*, and *MAPK6* correlated well indicating a non-stressed state of the plants. Then increasing the NaCl concentration to 50 mM the *NHX1* genes were activated inducing the vacuolar compartmentalization of Na and building up a new osmotic balance based on Na stores along with K which together maintained a largely unchanged water potential in the leaves. Further increasing the NaCl concentration, in the Na100 group, the efficient SOS system switched on to regulate cellular Na levels by removing Na to the apoplast (Carden et al., 2003). With the further increasing NaCl concentration, a new set of genes was activated to protect and repair the damaged cellular structures and/or readjust homeostatic balance (*PAO*, *HSP70*, *HSA1*, *CHS*, *PSBO*, and *PSBD*).

Sequential gene expression induced by increasing NaCl concentration provides a feasible explanation for the observed changes and underlines the tolerance of Szarvasi-1 energy grass to salinity. However, it should be noted that structural differences in the proteins and post-translational modifications in tolerant vs nontolerant varieties that were not studied in this work may also play an important role in salinity tolerance mechanisms (Assaha et al., 2017).

5. Conclusions

In this study, a comprehensive approach was applied to test the salinity tolerance of Szarvasi-1 energy grass. The activation and deactivation of specific genes inducing, regulating, and maintaining adequate responses to increasing NaCl concentration could be evaluated by PCA in relation to matrices of physiological and ionomical parameters. We have concluded that vacuolar compartmentalization was prevalent at moderate Na levels while it was replaced by Na removal (SOS1 activation) under higher Na concentrations. The highest, Na200 treatment well correlated with cellular repair mechanisms such as the heat shock proteins and the protection of the photosynthetic apparatus. These findings suggest that Szarvasi-1 energy grass is able to tolerate moderate salinity stress, and its responses to increasing NaCl levels exhibit a clear representation of genetic regulation behind the physiological behavior. The results may be exploited to evaluate salt tolerance of other (grass) species to be cultivated in moderately saline environments. Finally, the comprehensive approach for the studying of salinity stress responses proved to be highly informative to understand plant adaptation and should be applied in case of other stresses.

CRedit authorship contribution statement

Vitor Arcoverde Cerveira Sterner: Writing – original draft, Visualization, Formal analysis. **Kristóf Jobbágy:** Visualization, Formal analysis. **Brigitta Tóth:** Formal analysis. **Szabolcs Rudnóy:** Conceptualization. **Gyula Sipos:** Writing – review & editing, Conceptualization. **Ferenc Fodor:** Writing – review & editing, Supervision, Funding

acquisition, Conceptualization.

Declaration of competing interest

The authors declare that they have no known competing financial interests or personal relationships that could have appeared to influence the work reported in this paper.

Data availability

Data will be made available on request.

Acknowledgements

This work was supported by the National Research, Development and Innovation Office of Hungary, [NKFIH K-132241] and by the European Structural and Investment Funds, [VEKOP-2.3.3-15-2016-00008]. The authors are grateful to Dr. Adam Solti for critical revision of the manuscript.

Supplementary materials

Supplementary material associated with this article can be found, in the online version, at doi:10.1016/j.stress.2024.100572.

References

- Abdel Latef, A.A.H., Mostofa, M.G., Rahman, M.M., Abdel-Farid, I.B., Tran, L.S.P., 2019. Extracts from yeast and carrot roots enhance maize performance under seawater-induced salt stress by altering physio-biochemical characteristics of stressed plants. *J. Plant Growth Regul.* 38, 966–979. <https://doi.org/10.1007/s00344-018-9906-8>.
- Augustine, S.M., Narayan, J.A., Syamaladevi, D.P., Appunu, C., Chakravarthi, M., Ravichandran, V., Subramonian, N., 2015. *Erianthus arundinaceus* HSP70 (EaHSP70) overexpression increases drought and salinity tolerance in sugarcane (*Saccharum spp. hybrid*). *Plant Sci.* 232, 23–34. <https://doi.org/10.1016/j.plantsci.2014.12.012>.
- Assaha, D.V.M., Ueda, A., Saneoka, H., Al-Yahyai, R., Yaish, M.W., 2017. The role of Na⁺ and K⁺ transporters in salt stress adaptation in glycophytes. *Front. Physiol.* 8 <https://doi.org/10.3389/fphys.2017.00509>.
- Belkhdja, R., Morales, F., Quílez, R., López-Millán, A.F., Abadía, A., Abadía, J., 1998. Iron deficiency causes changes in chlorophyll fluorescence due to the reduction in the dark of the Photosystem II acceptor side. *Photosynth. Res.* 56, 265–276. <https://doi.org/10.1023/A:1006039917599>.
- Blumwald, E., Aharon, G.S., Apse, M.P., 2000. Sodium transport in plant cells. *Biochimica et Biophysica Acta (BBA) - Biomembranes* 1465, 140–151. [https://doi.org/10.1016/S0005-2736\(00\)00135-8](https://doi.org/10.1016/S0005-2736(00)00135-8).
- Breckle, S.W., 2002. Salinity, halophytes and salt affected natural ecosystems. *Environ. - Plants - Mole.* 53–77. https://doi.org/10.1007/0-306-48155-3_3.
- Carden, D.E., Walker, D.J., Flowers, T.J., Miller, A.J., 2003. Single-cell measurements of the contributions of cytosolic Na⁺ and K⁺ to salt tolerance. *Plant Physiol.* 131, 676–683. <https://doi.org/10.1104/PP.011445>.
- Chen, Z., Pottosin, I.I., Cuin, T.A., Fuglsang, A.T., Tester, M., Jha, D., Zepeda-Jazo, I., Zhou, M., Palmgren, M.G., Newman, I.A., Shabala, S., 2007. Root plasma membrane transporters controlling K⁺/Na⁺ homeostasis in salt-stressed barley. *Plant Physiol.* 145, 1714–1725. <https://doi.org/10.1104/PP.107.110262>.
- Csete, S., Stranczinger, S., Szalontai, B., Farkas, A., W, R., Salamon-Albert, E., Kocsis, M., Továri, P., Vojtela, T., Dezsó, J., Walcz, I., Janowszky, Zs., Janowszky, J., Borhidi, A., 2011. Tall wheatgrass cultivar Szarvasi-1 (*Elymus elongatus* Subsp. *Ponticus* cv. Szarvasi-1) as a potential energy crop for semi-arid lands of Eastern Europe. In: Nayeripour, M. (Ed.), Sustainable growth and applications in re-newable energy sources. In Tech, pp. 269–294. <https://doi.org/10.5772/26790>.
- Dao, T.T.H., Linthorst, H.J.M., Verpoorte, R., 2011. Chalcone synthase and its functions in plant resistance. *Phytochemistry Reviews* 10, 397–412. <https://doi.org/10.1007/s11101-011-9211-7>.
- Füzy, A., Kovács, R., Cseresnyés, I., Parádi, I., Szili-Kovács, T., Kelemen, B., Rajkai, K., Takács, T., 2019. Selection of plant physiological parameters to detect stress effects in pot experiments using principal component analysis. *Acta Physiol. Plant.* 41, 0. <https://doi.org/10.1007/s11738-019-2842-9>.
- Glenn, E.P., Brown, J.J., Blumwald, E., 1999. Salt tolerance and crop potential of halophytes. *CRC Crit. Rev. Plant. Sci.* 18, 227–255. <https://doi.org/10.1080/07352689991309207>.
- Gorham, J., Bristol, A., Young, E.M., Jonesh, R.G.W., Kashour, G., 1990. Salt Tolerance in the Triticeae: K/Na Discrimination in Barley. *J. Exp. Bot.* 41, 1095–1101. <https://doi.org/10.1093/JXB/41.9.1095>.

- Guo, R., Shi, L.X., Yan, C., Zhong, X., Gu, F.X., Liu, Q., Xia, X., Li, H., 2017. Ionic and metabolic responses to neutral salt or alkaline salt stresses in maize (*Zea mays* L.) seedlings. *BMC Plant Biol.* 17, 1–13. <https://doi.org/10.1186/s12870-017-0994-6>.
- Heath, R.L., Packer, L., 1968. Photoperoxidation in isolated chloroplasts. I. Kinetics and stoichiometry of fatty acid peroxidation. *Arch. Biochem. Biophys.* 125, 189–198. [https://doi.org/10.1016/0003-9861\(68\)90654-1](https://doi.org/10.1016/0003-9861(68)90654-1).
- Higgins, D.G., Heringa, J., 2000. T-Coffee: a novel method for fast and accurate multiple sequence alignment. *J. Mol. Biol.* 302, 205–217. <https://doi.org/10.1006/jmbi.2000.4042>.
- Ibrahimova, U., Kumari, P., Yadav, S., Rastogi, A., Antala, M., Suleymanova, Z., Ziveak, M., Tahjib-Ul-Arif, M., Hussain, S., Abdelhamid, M., Hajihashemi, S., Yang, X., Brestic, M., 2021. Progress in understanding salt stress response in plants using biotechnological tools. *J. Biotechnol.* 329, 180–191. <https://doi.org/10.1016/j.jbiotec.2021.02.007>.
- Isayenkov, S.V., Maathuis, F.J.M., 2019. Plant salinity stress: many unanswered questions remain. *Front. Plant Sci.* 10, 80. <https://doi.org/10.3389/fpls.2019.00080>.
- Kiani-Pouya, A., Rasouli, F., Rabbi, B., Falakboland, Z., Yong, M., Chen, Z.H., Zhou, M., Shabala, S., 2020. Stomatal traits as a determinant of superior salinity tolerance in wild barley. *J. Plant Physiol.* 245, 153108. <https://doi.org/10.1016/j.jplph.2019.153108>.
- Kiarash, J.G., Wilde, H.D., Amirmahani, F., Moemeni, M.M., Zaboli, M., Nazari, M., Moosavi, S.S., Jamalvandi, M., 2019. Selection and validation of reference genes for normalization of qRT-PCR gene expression in wheat (*Triticum durum* L.) under drought and salt stresses. *J. Genetics* 97, 1433–1444. <https://doi.org/10.1007/s12041-018-1042-5>.
- Kolberg, F., Tóth, B., Rana, D., Arcoverde Cerveira Sterner, V., Gerényi, A., Solti, Á., Szalóki, I., Sipos, G., Fodor, F., 2022. Iron status affects the zinc accumulation in the biomass plant Szarvasi-1. *Plants* 11, 3227. <https://doi.org/10.3390/plants11233227>.
- Li, C.H., Wang, G., Zhao, J.L., Zhang, L.Q., Ai, L.F., Han, Y.F., Sun, D.Y., Zhang, S.W., Sun, Y., 2014. The receptor-like kinase SIT1 mediates salt sensitivity by activating MAPK3/6 and regulating ethylene homeostasis in rice. *Plant Cell* 26, 2538–2553. <https://doi.org/10.1105/tpc.114.125187>.
- Li, Q.Y., Niu, H.B., Yin, J., Wang, M.B., Shao, H.B., Deng, D.Z., Chen, X.X., Ren, J.P., Li, Y.C., 2008. Protective role of exogenous nitric oxide against oxidative-stress induced by salt stress in barley (*Hordeum vulgare*). *Colloids. Surf. B Biointerfaces.* 65, 220–225. <https://doi.org/10.1016/j.colsurfb.2008.04.007>.
- Liu, H.C., Liao, H.T., Charng, Y.Y., 2011. The role of class A1 heat shock factors (HSFA1a) in response to heat and other stresses in Arabidopsis. *Plant Cell Environ.* 34, 738–751. <https://doi.org/10.1111/j.1365-3040.2011.02278.x>.
- Luna, C., García Seffino, L., Arias, C., Taleisnik, E., 2000. Oxidative stress indicators as selection tools for salt tolerance. *Plant Breed.* 119, 341–345. <https://doi.org/10.1046/j.1439-0523.2000.00504.x>.
- Martyniak, D., Żurek, G., Prokopiuk, K., 2017. Biomass yield and quality of wild populations of tall wheatgrass [*Elymus elongatus* (Host.) Runemark]. *BioMass BioEnergy* 101, 21–29. <https://doi.org/10.1016/j.biombioe.2017.03.025>.
- Maathuis, F.J.M., Ahmad, I., Patishtan, J., 2014. Regulation of Na⁺ fluxes in plants. *Front. Plant Sci.* 5, 467. <https://doi.org/10.3389/fpls.2014.00467>.
- Montero-Barrientos, M., Hermosa, R., Cardoza, R.E., Gitierez, S., Nicolas, C., Monte, E., 2010. Transgenic expression of the Trichoderma harzianum hsp70 gene increases Arabidopsis resistance to heat and other abiotic stresses. *J. Plant Physiol.* 167, 659–665. <https://doi.org/10.1016/j.jplph.2009.11.012>.
- Müller, B., Sterner, V.A.C., Papp, L., May, Z., Orlóci, L., Gyuricza, C., Sági, L., Solti, Á., Fodor, F., 2022. Alkaline salt tolerance of the biomass plant *Arundo donax*. *Agronomy* 12, 1589. <https://doi.org/10.3390/agronomy12071589>.
- Munns, R., Tester, M., 2008. Mechanisms of salinity tolerance. *Annu Rev. Plant Biol.* 59, 651–681. <https://doi.org/10.1146/ANNUREV.ARPLANT.59.032607.092911>.
- Ondrasek, G., Rathod, S., Manohara, K.K., Gireesh, C., Anantha, M.S., Sakhare, A.S., Parmar, B., Yadav, B.K., Bandumula, N., Raihan, F., Zielnińska-Chmielewska, A., Meriño-Gergichevich, C., Reyes-Díaz, M., Khan, A., Panfilova, O., Fuentealba, A.S., Romero, S.M., Nabil, B., Wan, C., Shepherd, J., Horvatinec, J., 2022. Salt stress in plants and mitigation approaches. *Plants* 11, 717. <https://doi.org/10.3390/PLANTS11060717>.
- Ouerghi, Z., Cormic, G., Roudani, M., Ayadi, A., Brulfert, J., 2000. Effect of NaCl on Photosynthesis of Two Wheat Species (*Triticum durum* and *T. aestivum*) Differing in their Sensitivity to Salt Stress. *J. Plant Physiol.* 156, 335–340. [https://doi.org/10.1016/S0176-1617\(00\)80071-1](https://doi.org/10.1016/S0176-1617(00)80071-1).
- Paolacci, A.R., Tanzarella, O.A., Porceddu, E., Ciaffi, M., 2009. Identification and validation of reference genes for quantitative RT-PCR normalization in wheat. *BMC Mol. Biol.* 10, 11. <https://doi.org/10.1186/1471-2199-10-11>.
- Petrussa, E., Braidot, E., Zancani, M., Peresson, C., Bertolini, A., Patui, S., Vianello, A., 2013. Plant flavonoids—biosynthesis, transport and involvement in stress responses. *International J. Mol. Sci.* 14, 14950–14973. <https://doi.org/10.3390/ijms140714950>.
- Pfaffl, M.W., 2004. Relative quantification. In: Dorak, T. (Ed.), *Real-time PCR*. International University Line, pp. 63–82.
- Podani, J., 2000. *Introduction to the exploration of multivariate biological data*. Backhuys Publishers.
- Porra, R.J., Thompson, W.A., Kriedemann, P.E., 1989. Determination of accurate extinction coefficients and simultaneous equations for assaying chlorophylls a and b extracted with four different solvents: verification of the concentration of chlorophyll standards by atomic absorption spectroscopy. *Biochimica et Biophysica Acta (BBA) - Bioenerget.* 975, 384–394. [https://doi.org/10.1016/S0005-2728\(89\)80347-0](https://doi.org/10.1016/S0005-2728(89)80347-0).
- Ramakers, C., Ruijter, J.M., Deprez, R.H.L., Moorman, A.F.M., 2003. Assumption-free analysis of quantitative real-time polymerase chain reaction (PCR) data. *Neurosci. Letters* 339, 62–66. [https://doi.org/10.1016/S0304-3940\(02\)01423-4](https://doi.org/10.1016/S0304-3940(02)01423-4).
- Rév, A., Tóth, B., Solti, Á., Sipos, G., Fodor, F., 2017. Responses of Szarvasi-1 energy grass to sewage sludge treatments in hydroponics. *Plant Physiol. Biochem.* 118, 627–633. <https://doi.org/10.1016/j.plaphy.2017.07.027>.
- Saccò, M., White, N.E., Harrod, C., Salazar, G., Aguilar, P., Cubillos, C.F., Meredith, K., Baxter, B.K., Oren, A., Anufrieva, E., Shadrin, N., Marambio-Alfaro, Y., Bravo-Naranjo, V., Allentoft, M.E., 2021. Salt to conserve: a review on the ecology and preservation of hypersaline ecosystems. *Biolog. Rev.* 96, 2828–2850. <https://doi.org/10.1111/BRV.12780>.
- Sanchez-Aguayo, I., Rodriguez-Galan, J.M., Garcia, R., Torreblanca, J., Pardo, J.M., 2004. Salt stress enhances xylem development and expression of S-adenosyl-L-methionine synthase in lignifying tissues of tomato plants. *Planta* 220, 278–285. <https://doi.org/10.1007/s00425-004-1350-2>.
- Shakirova, F.M., Sakhabutdinova, A.R., Bezrukova, M.V., Fatkhutdinova, R.A., Fatkhutdinova, D.R., 2003. Changes in the hormonal status of wheat seedlings induced by salicylic acid and salinity. *Plant Sci.* 164, 317–322. [https://doi.org/10.1016/S0168-9452\(02\)00415-6](https://doi.org/10.1016/S0168-9452(02)00415-6).
- Sievers, F., Higgins, D.G., 2021. The clustal omega multiple alignment package. *Meth. Mol. Biol.* 2231, 3–16. https://doi.org/10.1007/978-1-0716-1036-7_1.
- Sipos, G., Solti, Á., Czech, V., Vashegyi, I., Tóth, B., Cseh, E., Fodor, F., 2013. Heavy metal accumulation and tolerance of energy grass (*Elymus elongatus* subsp. ponticus cv. Szarvasi-1) grown in hydroponic culture. *Plant Physiol. Biochem.* 68, 96–103. <https://doi.org/10.1016/j.plaphy.2013.04.006>.
- Sóti, A., Ounoki, R., Kósa, A., Mysliwa-Kurdziel, B., Sárvári, É., Solymosi, K., 2023. Ionic, not the osmotic component, is responsible for the salinity-induced inhibition of greening in etiolated wheat (*Triticum aestivum* L. cv. Mv Bérés) leaves: a comparative study. *Planta* 258, 102. <https://doi.org/10.1007/s00425-023-04255-4>.
- Spalding, E.P., Hirsch, R.E., Lewis, D.R., Qi, Z., Sussman, M.R., Lewis, B.D., 1999. Potassium uptake supporting plant growth in the absence of AKT1 channel activity inhibition by ammonium and stimulation by sodium. *J. Gen. Physiol.* 113, 909–918. <https://doi.org/10.1085/JGP.113.6.909>.
- Tattini, M., Remorini, D., Pinelly, P., Agati, G., Saracini, E., Traversi, M.L., Massai, R., 2006. Morpho-anatomical, physiological and biochemical adjustments in response to root zone salinity stress and high solar radiation in two Mediterranean evergreen shrubs, *Myrtus communis* and *Pistacia lentiscus*. *New Phytol.* 170, 779–794. <https://doi.org/10.1111/j.1469-8137.2006.01723.x>.
- Flowers, T.J., Troke, P.F., Yeo, A.R., 2003. The mechanism of salt tolerance in halophytes. *Annu. Rev. Plant Physiol.* 28, 89–121. <https://doi.org/10.1146/ANNUREV.PP.28.060177.000513>.
- Untergasser, A., Cutcutache, I., Koressaar, Y.J., Faircloth, B.C., Remm, M., Rozen, S.G., 2012. Primer3 - new capabilities and interfaces. *Nucleic Acids Res.* 40, 1–12. <https://doi.org/10.1093/nar/gks596>.
- Vashegyi, I., Cseh, E., Lévai, L., Fodor, F., 2011. Chelator-enhanced lead accumulation in agropyron elongatum cv. Szarvasi-1 in hydroponic culture. *Int. J. Phytoremed.* 13, 302–315. <https://doi.org/10.1080/15226514.2010.483261>.
- Wani, S.H., Kumar, V., Khare, T., Guddimalli, R., Parveda, M., Solymosi, K., Suprasanna, P., Kavi Kishor, P.B., 2020. Engineering salinity tolerance in plants: progress and prospects. *Planta* 251, 76. <https://doi.org/10.1007/s00425-020-03366-6>.
- Wegner, L.H., Raschke, K., 1994. Ion channels in the xylem parenchyma of barley roots (a procedure to isolate protoplasts from this tissue and a patch-clamp exploration of salt passageways into xylem vessels. *Plant Physiol.* 105, 799–813. <https://doi.org/10.1104/PP.105.3.799>.
- Wu, D., Shen, Q., Cai, S., Chen, Z.H., Dai, F., Zhang, G., 2013. Ionic responses and correlations between elements and metabolites under salt stress in wild and cultivated barley. *Plant Cell Physiol.* 54, 1976–1988. <https://doi.org/10.1093/pcp/pct134>.